Proc. Natl. Sci. Counc. ROC(A)
Vol. 22, No. 1, 1998. pp. 35-47

Experimental Dynamic Walking of a Seven Degrees-of-Freedom Biped Robot

CHING-LONG SHIH AND CHENG-PING PO

Department of Electrical Engineering
National Taiwan Institute of Technology
Taipei, Taiwan, R.O.C.

(Received November 28, 1996; Accepted July 31, 1997)

ABSTRACT

The motivation of this work was to synthesize a smooth and energy-optimized walking pattern for a seven degrees-of-freedom biped robot walking on an even floor. The biped's walk is realized by tracking control of the planned trajectory. The biped robot achieved walk initiation and continuous walking back and forth, and the biped can walk with a speed of 20 cm/second on even floors. The contributions of this work are: (1) the results of experiments on a seven degrees-of-freedom prototype biped, which is capable of walking in a dynamically stable manner, are presented, (2) the synthesis of an energy-optimized walking gait is proposed, and (3) the reasoning behind the local PD feedback loop justifies satisfactory performance.

Key Words: biped robot, dynamically stable walking, motion control

I. Introduction

For statically stable locomotion, the walking trajectory of a legged robot is characterized by a center-of-gravity (cg) which is within its support region, that is, the convex hull consisting of its supporting foot or feet. Moreover, the robot must move slowly so that inertial effects from reciprocating legs do not disturb its balance. Statically stable walking has been widely studied in walikng robots, with four or more legs, in which at least three feet are in contact with the ground at any time. The stability of such slow-moving, multilegged walkers can be adequately quantified by using static analysis. On the other hand, for dynamically stable locomotion, the center of gravity may lie outside of the support region. In this case, the legged robot requires a higher speed to recover itself from an unstable state; otherwise, it may fall down. Most biped research has focused on building a robot capable of dynamic walking on an even floor. In particular, several prototype biped robots that walk in a dynamically stable manner have been developed at Japanese universities. The control of biped walking machines remains a challenge due to the high degree of complexity, organization, and efficiency needed to maintain balance.

The following is a review of the biped research in dynamic walking. Miyazaki and Arimoto (1980) proposed original reduced-order models that have quantitative relations with the original equations of motion. By setting a simple reference signal function for each controller and using the function repeatedly for each step, stable walking was achieved. Miura and Shimoyama (1984) conducted stability analysis by using an inverted pendulum and developed two biped robots that could walk in a dynamically stable mode. Mita *et al.* (1984) aimed to realize dynamic biped locomotion by using modern control theory, especially optimal regulator theory, and conducted plane walking experiments. Furusho and Masubuchi (1986) experimented with a walking biped, in which each joint was provided with a local high-gain position feedback control. Zheng and Sias (1988) discussed the design of two biped robots, SD-1 and SD-2, and showed that stable dynamic walk could be realized as long as the landing foot was properly positioned. Furusho and Sano (1990) achieved smooth 3D walking by using a sensor-based control on a biped with nine links. They employed a method to control walking by dividing it into motions in the sagittal plane and the lateral plane. The motion in the lateral plane had a regulator problem with two equilibrium states. For motion in the sagittal plane, they adjusted the body speed so that it was close to the smooth speed function given in advance by controlling the ankle torque. The sole and ankle driving actuators underwent force/torque

feedback control that was based on the sensor information.

Li *et al.* (1991) used the zero-moment-point (Vukobratovic, 1973) as a criterion in order to distinguish the stability of walking for the biped robot WL-12RIII. The assignment of degrees of freedom for their robot was as follows: each of the two hips, the two knees, and the two ankles had one rotational degree of freedom on the pitch axis. The body had three degrees of freedom in the pitch, roll, and yaw axes. Walking was realized by controlling the body's motion to compensate for the biped walking according to the measured zero-moment-point. Kajita *et al.* (1992) used the term "potential energy conserving orbit" to describe a particular class of trajectories of an ideal biped model. Based on these properties, control laws were formulated for walk initiation, walk continuation, and walk termination. To make their robot legs lighter, four dc motors were mounted on the body, and the legs had parallel link structures which helped the biped walk at an average speed of 20 cm/s. Grishin *et al.* (1994) designed a light walking vehicle with two telescopic legs, driven by two dc motors. The robot's feet extended beyond the center of the body in the frontal plane, and an adaptive algorithm was used to control the vehicle locomotion. Shih (1996a) built a biped robot (named BR-1) capable of statically and dynamically stable walking on an even floor. Because the body and swing leg speeds were not small at the end of a walking cycle and the impact effect was not considered, the biped's walking was not smooth enough. This was because the planned trajectories for the body and swing foot were hyperbolic functions.

To implement a controller for a biped robot, it is necessary to generate an admissible and optimal trajectory for use as a reference input. Previous methods for synthesizing biped walking trajectories have included recording human kinematic data, using finite state machines, merging trajectory control with feedback control laws, and generating gaits from the passive interaction of gravity and inertia. This article describes the design of a biped robot, its kinematics, dynamics, energy-optimized gait synthesis, and its implementation. This study is based on a practical biped robot BR-1, and the goal is to synthesize efficient and energy-optimized walking patterns for floor walking by means of proper positioning of the biped's body and its two feet. The assumptions of this study are (1) the feet are rigid, (2) each supporting foot is in flat contact with a hard surface terrain, and (3) there is enough frictional force to prevent slippage between the foot and the floor during walking.

The outline of the paper is as follows. The mathematic models of the biped robot, including the design concepts, dynamics, static balance conditions, energy-consumption, and impact effects, are derived in Section II. The plan for the dynamic walking gait of the biped BR-1 on an even floor is discussed in Section III. The PD motion control law of the biped walking is proposed in Section IV. The implementation of the biped's control system and its experimental walking results are summarized in Section V.

II. Biped Robot and Model

The biped robot has two rotational joints on the hip and the ankle joint as well as one variable-length knee on each leg. In addition, one actuator is associated with the body to translate a balance weight in the lateral motion. Seven DC servo motors are employed as actuators. The biped structure is both back-and-forth and left-and-right symmetric. Therefore, the backward motion can be planned by reversing the sequence of the forward motion. Compared to anthropomorphic biped robots, the biped robot has simpler kinematics and dynamics.

The biped robot consists of the moving weight body, two legs, and two feet. The feet are designed to be lighter than the other parts of the biped robot; therefore, the weight of the robot feet is negligible. To simplify the analysis of the dynamics of the biped system, each leg is replaced by two point masses at the ankle joint and the hip joint. The idea here is to represent the leg with two point masses which are placed where the position, velocity, and accelerations can easily be determined. Physically, the speed reducers and DC servo motors are considerably heavier than the links of the leg; thus, the mass of the leg can be simplified as two point masses at the ankle joint and the hip joint.

The balance weight is designed to maintain the projection of the center of gravity within the supporting foot during the single-support phase for statically stable walking. With the moving weight, we do not need to have the feet cross the center line and do not need to have a supporting mechanism to prevent the robot from falling over laterally. Moreover, the heavier the moving weight is, the smaller is the foot needed. Thus, the moving weight plays an important role in maintaining balance and improving the speed of the biped robot because a large foot may cause interference between the two feet, and a large foot will force the biped to walk at a slow speed.

The variable-length leg is designed to replace the function of the knee joint. With the variable-length leg, the biped can travel on a rough terrain, such as

stairs. To climb stairs, the biped's body and its one leg can move upwards by simply utilizing the variable-length knees. After that, the walking cycle can be treated as level walking.

Now, we shall model the seven degrees-of-freedom biped robot BR-1 based on the single-support case in which one leg is stationary on the floor. Figure 1 shows a schematic representation of the biped

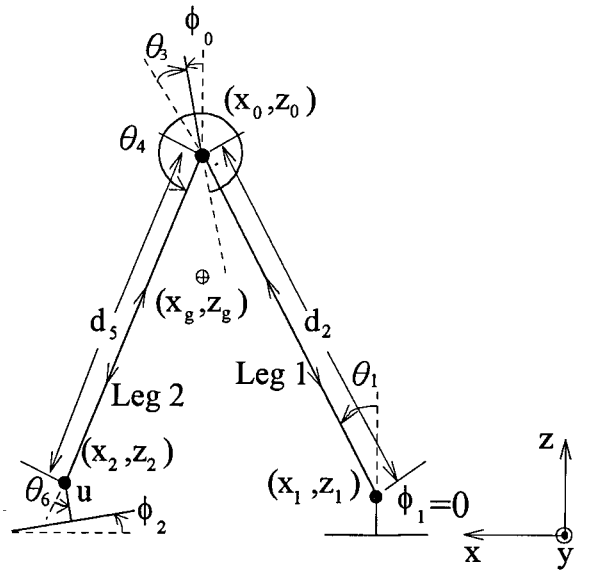

(a) sagittal plane

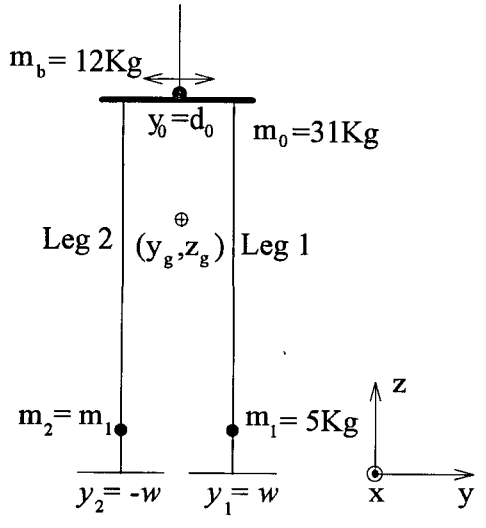

(b) frontal plane

Fig. 1. The kinematic model of the biped BR-1 in (a) the sagittal plane and (b) the frontal plane, where (x_g, y_g, z_g) denotes the center of gravity of the biped robot. The angle is positive if ccw and negative if cw.

model in the sagittal plane (x-z plane) and in the frontal plane (y-z plane). The origin of the base reference coordinate is located at the vertical projection of the center of the body in the ground plane when the biped is in its initial configuration. Because the legs are constrained to swing in the sagittal plane, rotational motion of the biped BR-1 is allowed only in the sagittal plane.

The position of the biped relative to the supporting foot can be uniquely specified by the joint space vector $\boldsymbol{q}$ (see Fig. 1),

$$\boldsymbol{q}=[q_0, q_1, \ldots, q_6]^T=[d_0, \theta_1, d_2, \theta_3, \theta_4, d_5, \theta_6]^T,$$

where

d_0: location of the balance weight,

θ_1: angle of the hip joint of Leg 1,

d_2: length of Leg 1 from the hip joint to the ankle joint,

θ_3: angle of the ankle joint of Leg 1,

θ_4: angle of the hip joint of Leg 2,

d_5: length of Leg 2 from the hip joint to the ankle joint,

θ_6: angle of the ankle joint of Leg 2,

and by the joint torque/force vector given by $\boldsymbol{\tau}$:

$$\boldsymbol{\tau}=[\tau_0, \tau_1, \ldots, \tau_6]^T.$$

The dynamic equation in the single support phase can be derived by using the Lagrangian formulation and can be written as

$$\boldsymbol{H}(\boldsymbol{q})\ddot{\boldsymbol{q}}+\boldsymbol{C}(\boldsymbol{q},\dot{\boldsymbol{q}})\dot{\boldsymbol{q}}+\boldsymbol{g}(\boldsymbol{q})=\boldsymbol{\tau}. \quad (1)$$

Here, $\boldsymbol{H}(\boldsymbol{q})$ is a 7×7 symmetric positive-definite matrix containing mass and inertia elements, $\boldsymbol{C}(\boldsymbol{q},\dot{\boldsymbol{q}})\dot{\boldsymbol{q}}$ is a 7×1 vector containing centrifugal and Coriolis terms, and $\boldsymbol{g}(\boldsymbol{q})$ is a 7×1 vector of gravity terms.

Analysis of the biped motion in terms of the body and both feet makes it possible to ease the formulation and interpretation. The operation space position vector $\boldsymbol{p}$,

$$\boldsymbol{p}=[p_0, p_1, \ldots, p_6]^T=[y_0, x_0, z_0, \phi_0, x_2, z_2, \phi_2]^T,$$

is defined by

$$\boldsymbol{p}=\begin{bmatrix} y_0 \\ x_0 \\ z_0 \\ \phi_0 \\ x_2 \\ z_2 \\ \phi_2 \end{bmatrix}=\begin{bmatrix} y_1-w+d_0 \\ x_1+d_2\sin(\phi_1+\theta_1) \\ z_1+d_2\cos(\phi_1+\theta_1) \\ \phi_1+\theta_1+\theta_3 \\ x_0-d_5\sin(\phi_0+\theta_4) \\ z_0-d_5\cos(\phi_0+\theta_4) \\ \phi_0+\theta_4+\theta_6 \end{bmatrix} \tag{2}$$

where

$\boldsymbol{x}_0=[x_0, y_0, z_0]^T$: the location of the balance weight,

$\boldsymbol{x}_1=[x_1, y_1, z_1]^T$: the location of Foot 1,

$\boldsymbol{x}_2=[x_2, y_2, z_2]^T$: the location of Foot 2,

ϕ_0, ϕ_1, ϕ_2 : the pitch angle of the body, Foot 1 and Foot 2,

and

w: half of the width of the biped.

It is noted that the mapping between $\boldsymbol{p}$ and $\boldsymbol{q}$ is a one-to-one mapping, and that the Jacobian matrix $\boldsymbol{J}$,

$$\boldsymbol{J}=\frac{\partial \boldsymbol{p}}{\partial \boldsymbol{q}} \tag{3}$$

is non-singular (Shih, 1996a).

Because the speed reducers and DC servo motors are considerably heavier than the links of the leg and the frame of the body platform, we assume that the mass of the biped is distributed as four units: the balance weight, the body platform, and two feet. The dynamic equation of the biped in Eq. (1) can be written in the operation space (Shih, 1996a) as:

$$\boldsymbol{M}\ddot{\boldsymbol{p}}+\boldsymbol{G}=\boldsymbol{f}=\boldsymbol{J}^{-T}\tau, \tag{4}$$

where

$\boldsymbol{M}=\text{diag}\{m_b, m_0, m_0, I_0, m_2, m_2, I_2\}$,

$\boldsymbol{G}=[0\ 0\ m_1 g\ 0\ 0\ m_0 g\ 0]^T$,

m_b: the mass of the balance weight,

m_0: the mass of the body including the balance weight,

m_1, m_2: the masses of Foot 1 and Foot 2,

I_0, I_1, I_2: the moment of inertia (in y-axis) of the biped body, Foot 1 and Foot 2,

and

$\boldsymbol{f}=[f_0, f_1, \ldots, f_6]^T$: the operation space generalized torque/force vector.

The conditions for balancing is an important factor in designing a feasible gait pattern, especially for high speed locomotion. Aside from the frictional force, the forces acting on the biped include the gravity force, the inertial force, the inertial moment, and the ground reaction force. Actually, the biped interacts with the ground through a planar surface. Most of the time, the ankle joint motor has to generate a torque to support biped locomotion. This torque must be resisted by the ground and the supporting foot.

The vertical reaction force, N_z, must be positive during the whole walking cycle so that the foot remains on the floor, i.e.,

$$N_z>0.$$

The absolute horizontal reaction force, $\sqrt{N_x^2+N_y^2}$, must not be so large that the foot slides; therefore, it is required that

$$\sqrt{N_x^2+N_y^2}\le\mu N_z. \tag{5}$$

The reaction moments T_x and T_y must be resisted by the normal ground reaction force N_z of the supporting foot to prevent the biped from falling down (Fig. 2). Hence,

$$N_z(y_1-d)\le T_x\le N_z(y_1+d) \tag{6}$$

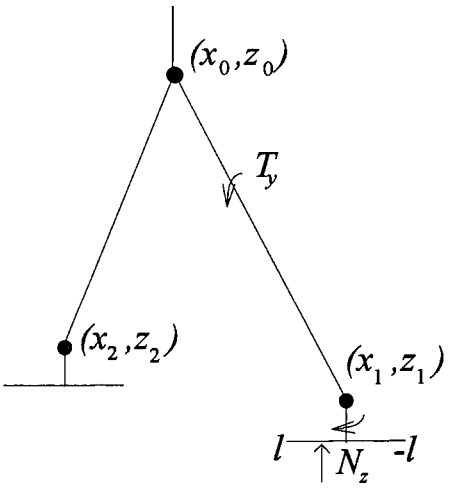

Fig. 2. The static balance condition in the single-support phase.

and

$$-N_z(x_1+l)\le T_y\le -N_z(x_1-l), \tag{7}$$

where

$$T_x = y_1 m_1 g + y_b m_b(\ddot{z}_0+g) + y_2 m_2(\ddot{z}_2+g) - z_0 m_b \ddot{y}_b$$

$$T_y = z_0 m_0 \ddot{x}_0 + z_2 m_2 \ddot{x}_2 - x_0 m_0(\ddot{z}_0+g) - x_2 m_2(\ddot{z}_2+g) + I_0\ddot{\phi}_0 + I_2\ddot{\phi}_2$$

and

$2l\times 2d$ is the foot size.

In other words, the reaction moments T_x and T_y must not be so large that the foot lifts up from the floor.

The energy consumption or efficiency should also be considered an essential factor in designing a biped gait pattern. The average-energy-consumption function E, defined by

$$E = \frac{\int_0^T |\tau^T \dot{q}|dt}{S}, \tag{8}$$

is a division of the sum of the energy-consumption of all the joint actuators by the step distance S during one walking cycle. Note that the absolute value of the instantaneous power loss is used. The absolute value indicates that the power is actively consumed in dissipating this energy while the division of the step length in the function E allows gaits of different step lengths to be compared. The average-energy-consumption function E can also be evaluated in the operation space below:

$$E = \frac{\int_0^T |f^T \dot{p}|dt}{S} = \frac{\int_0^T |(M\ddot{p}+G)^T \dot{p}|dt}{S}. \tag{9}$$

Now, consider the impact phase that occurs at the end of the walking cycle at time $t=T$. This is assumed to be instantaneous, resulting in an abrupt change in the joint velocity due to the collision between the swing foot and the floor. Let the impact point between the swing foot and the floor be defined as below:

$$c(p) = \begin{bmatrix} x_2 - x_1 - S \\ z_2 \\ \phi_2 \end{bmatrix} = 0. \tag{10}$$

The dynamic equation of the biped under impact can be modeled as

$$M\ddot{p} + G = f + \frac{\partial c^T}{\partial p}\lambda, \tag{11}$$

where λ is the vector of the constraint forces applied to the new landing foot during impact. Integrating Eq. (11) in an infinitesimally short time interval $[T_-, T_+]$, we can derive the relation between the instantaneous velocity changes and the constraint forces λ. The positions and generalized forces f remain finite; therefore, we obtain

$$\Delta\dot{p} = \dot{p}(T_+) - \dot{p}(T_-) = M^{-1}\frac{\partial c^T}{\partial p}\int_{T_-}^{T_+}\lambda dt \tag{12}$$

and

$$\delta = \int_{T_-}^{T_+}\lambda dt = \left(\frac{\partial c}{\partial p}M^{-1}\frac{\partial c^T}{\partial p}\right)^{-1}\frac{\partial c}{\partial p}\Delta\dot{p}. \tag{13}$$

The vectors $\dot{p}(T_-)$ and $\dot{p}(T_+)$ represent the velocities immediately before and after impact, and the vector δ represents the magnitude of the external impulsive force. The instant joint velocity changes can then be obtained from

$$\left(\frac{\partial c}{\partial p}M^{-1}\frac{\partial c^T}{\partial p}\right)^{-1}\frac{\partial c}{\partial p}J\Delta\dot{q} = \delta, \tag{14}$$

where $\Delta\dot{q} = \dot{q}(T_+) - \dot{q}(T_-)$.

Specifically, the magnitude of the external impact forces is

$$\delta = \begin{bmatrix} \delta_x \\ \delta_z \\ \tau_y \end{bmatrix} = \begin{bmatrix} m_2\Delta\dot{x}_2 \\ m_2\Delta\dot{z}_2 \\ I_2\Delta\dot{\phi}_2 \end{bmatrix}. \tag{15}$$

If $|\delta_x| > \mu\delta_z$, then sliding occurs; therefore, it is required that

$$\delta_z > 0$$

and

$$|\delta_x| \le \mu\delta_z.$$

One simple way to satisfy the above inequality is to have a zero-forward-velocity (i.e. $\dot{x}_2(T_-)=0$) when the swing leg touches the floor. The impulsive moment τ_y must also not be so large that the heel or the toe lifts up from the floor, i.e.,

$$-\delta_z l \le \tau_y \le \delta_z l.$$

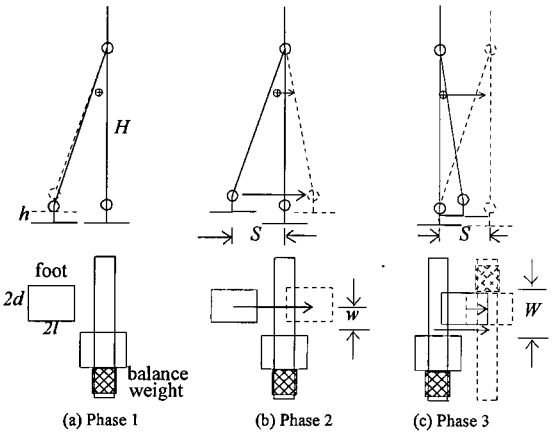

Fig. 3. The dynamic walking cycle of the biped BR-1 in three phases.

By constraining the swing foot in a fixed orientation (i.e. ϕ_2=0) and parallel to the walking floor, the above inequality is satisfied.

III. Walking Trajectory

In the following analysis, a walking cycle will be regarded as a period of continuous motion in which the biped is supported by one foot, followed by an instantaneous impact of the swing foot at the end of the cycle. After impact, the motion is the same as the start of the cycle except that the supporting foot becomes the swing foot and vice versa. For dynamic walking on an even plane, the walking cycle of the biped can be modeled in three phases, as shown in Fig. 3. During Phase 1, the swing leg lifts up above the ground. The swing foot moves forward above the ground in Phase 2. Finally, the body moves forward and the swing foot comes back to the ground in Phase 3. During Phase 3, the center of gravity leaves the supporting foot; this shift in the center of gravity actually is characteristic of a biped walking dynamically. Letting T_1, T_2, and T_3 be the time intervals for Phases 1, 2, and 3, respectively, the dynamic walking cycle T then consists of T_1, T_2, and T_3. The above walking pattern can be determined from a set of walking pattern parameters - they are the step size S, the body height H, the swing leg height h, the balance weight traveling distance $2W$, and the time intervals T_1, T_2, and T_3.

In fact, the motions of the biped body and the two feet follow an alternating move-and-rest pattern. Thus, piecewise cubic polynomials with zero velocity at both ends of the moving time interval are quite adequate for modeling the variations of the work space variables. Polynomials of third order are chosen so as to have minimum complexity to allow the positions and velocities at the two ends of a time interval to be freely allocated. The cubic trajectory for a variable $p(t)$ satisfying initial and final values, with rest at both ends of time interval T_P (i.e. $p(0)=p_s$, $p(T_p)=p_T$, and $\dot{p}(0)=\dot{p}(T_p)=0$), is

$$p(t)=2(p_s-p_T)\frac{t^3}{T_p^3}+3(p_T-p_S)\frac{t^2}{T_p^2}+p_S,$$

$$0\le t\le T_p. \tag{16}$$

The acceleration of $p(t)$ is a linear function, and its end values are

$$\ddot{p}(T_p)=6\frac{p_T-p_s}{T_p^2} \text{ and } \ddot{p}(T_p)=-\ddot{p}(0)=6\frac{p_s-p_T}{T_p^2}.$$

At the middle of the time interval T_p, we have

$$p(T_p/2)=\frac{p_s+p_T}{2},\ \dot{p}(T_p/2)=\frac{3(p_T-p_s)}{2T_p},$$

and $\ddot{p}(T_p/2)=0$,

where $p(t)$ reaches the half-way point and has maximum speed and zero acceleration. This particular type of trajectory is used as the basic trajectory for the work space position vector $\boldsymbol{p}$ to plan the biped's walking pattern. Also, note that

$$\int_0^{T_p}\left|\ddot{p}\dot{p}\right|dt=\dot{p}(T_p/2)^2, \tag{17}$$

and

$$\int_0^{T_p}\left|(\ddot{p}+g)\dot{p}\right|dt=\int_0^{T_p}\left|g\dot{p}\right|dt=g\left|p_T-p_s\right|, \tag{18}$$

and that these equalities will be utilized later to compute the average-energy-consumption function E.

It is assumed that the biped's body maintains a constant upright posture during motion, and that both feet stay parallel with the walking plane; therefore, $\phi_0=\phi_1=\phi_2=0$, and $\theta_1+\theta_3=\theta_4+\theta_6=0$. By default, Leg 1 is the supporting leg in the walking cycle; therefore, Leg 1 is stationary during the walking time interval T. Hence, $x_1=0$, $y_1=0$, and $z_1=0$ for simplicity. It is also desired that the body maintains a constant height, $z_0=H$, during walking. Foot 2 first lifts itself above the ground during Phase 1, moves forward at a constant height h in Phase 2, and then finally comes back to the ground at Phase 3. Thus, the trajectory of Foot 2 can be modeled as follows:

$$x_2(t)=\begin{cases} -S & 0\le t\le T_1 \\ -4S\dfrac{(t-T_1)^3}{(T_2+T_3-\delta T)^3}+6S\dfrac{(t-T_1)^2}{(T_2+T_3-\delta T)^2}-S & T_1<t\le T-\delta T \end{cases} \quad (19)$$

and

$$z_2(t)=\begin{cases} -2h\dfrac{t^3}{T_1^3}+3h\dfrac{t^2}{T_1^2} & 0\le t\le T_1 \\ h & T_1<t\le T_1+T_2 \\ 2h\dfrac{(t-T_1-T_2)^3}{T_3^3}-3h\dfrac{(t-T_1-T_2)^2}{T_3^2}+h & T_1+T_2<t\le T \end{cases} . \quad (20)$$

By using a small time interval δT, we can ensure that the swing leg has near zero-forward-velocity when it returns to the floor. Therefore, the effect of impact can be largely reduced. The biped body and the balance weight start to move at the beginning of Phase 3 by the following trajectories:

$$x_0(t)=\begin{cases} 0 & 0\le t\le T_1+T_2 \\ -2S\dfrac{(t-T_1-T_2)^3}{T_3^3}+3S\dfrac{(t-T_1-T_2)^2}{T_3^2} & T_1+T_2<t\le T \end{cases} \quad (21)$$

and

$$y_0(t)=\begin{cases} W-w & 0\le t\le T_1+T_2 \\ 4W\dfrac{(t-T_1-T_2)^3}{T_3^3}-6W\dfrac{(t-T_1-T_2)^2}{T_3^2}+W-w & T_1+T_2<t\le T \end{cases} . \quad (22)$$

After a series of manipulations, the average-energy-consumption function E can be derived as

$$E=\frac{1}{S}\left[\frac{9m_2S^2}{(T_2+T_3)^2}+\frac{9m_0}{4}\frac{S^2}{T_3^2}+9m_b\frac{W^2}{T_3^2}+2m_2gh\right]. \quad (23)$$

To determine a feasible walking pattern, several factors should be considered: they are the position and velocity constraints for work space vector $\boldsymbol{p}$, the static

balance conditions for the supporting foot, and the not-falling-down condition for the swing leg. The position constraints for the swing foot can only be checked at both ends of Phase 1. Recalling that the operation space trajectory reaches its highest speed at the middle of the move time interval, the speed constraints can only be checked at the middle of each phase. The static balance constraints in Inequalities (6) and (7) need to be checked at every transition of the three phases.

During Phase 3, the projection of the center of gravity moves out of the supporting foot, the body starts to fall, and the swing foot must reach the ground before the biped falls over. Therefore, the high speed of the biped must be maintained during Phase 3. The not-falling-down condition is complicated and not easily obtained. The joint motions in the supporting leg are very limited and may be considered to be zero. We may, therefore, consider the biped body as a 3D inverted pendulum during Phase 3. The increment of the potential energy, because the biped body maintains a constant height H, is

$$m_0 gH(1-\frac{H}{\sqrt{H^2+S^2}}). \tag{24}$$

The total kinetic energy of the biped motion during Phase 3 should equal the increment of the potential energy of the biped body; therefore, we obtain

$$m_0 gH(1-\frac{H}{\sqrt{H^2+S^2}})=\frac{9MS^2}{4T_3^2}+\frac{9m_bW^2}{T_3^2}. \tag{25}$$

This equality should be satisfied when the biped's pattern parameters are searched.

By minimizing the average-energy-consumption function E, subject to the position, velocity, and balance inequality constraints as well as the equality constraint Eq. (25) and an input speed constraint, $S/T_3=Constant$, we can obtain parameters for an energy-optimized biped walking pattern. Among the biped's walking parameters, the choice of the step size S and of the time interval T_3 are most critical to the success of the biped walk. The walking parameters H, h, and W can be chosen easily, and we let $2T_1=T_2=T_3$. We can then obtain the optimal values of the step size S and the time interval T_3 by using the graph method to impose the constraints on the contour plot of the average-energy-consumption function E in the S–T_3 plane. Taking the BR-1 biped robot as an example, and letting H=0.54 m, h=0.03 m, W=0.15 m, $2T_1=T_2=T_3$, δT=0.05 seconds, and S/T_3=0.25, the step size S and the time interval

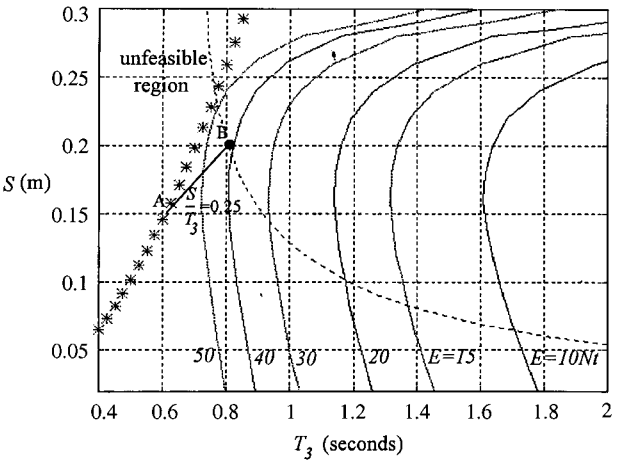

Fig. 4. A contour plot of the average-consumption function E in the S-T_3 plane. The solid line segment AB represents the input speed constraint, and the dashed line represents the equality constraint of Eq. (25). The energy-optimizing parameters are S=0.20 m and T_3=0.80 seconds.

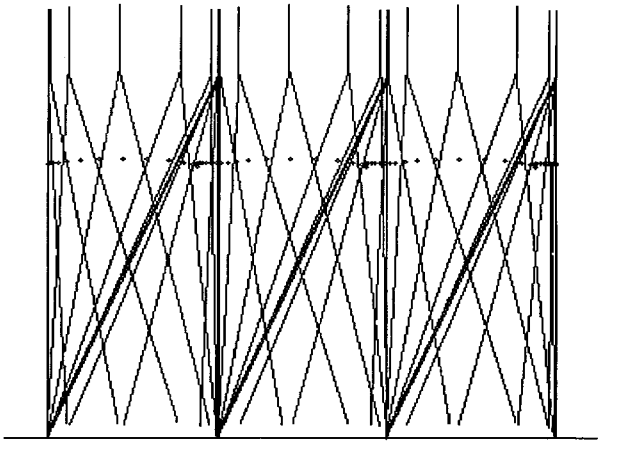

Fig. 5. Biped BR-1's motion sequence in the dynamic walking simulation. The small circles denote the center of gravity trajectory.

T_3 are determined by the following minimization problem:

Minimize

$$E=\frac{2.01}{ST_3^2}+\frac{83.25S}{T_3^2}$$

subject to equalities

$$\frac{94.5S^2+29.16}{T_3^2}=169.344(1-\frac{0.54}{\sqrt{0.2916+S^2}})$$

$$\frac{S}{T_3}=0.25$$

and inequalities

$$0 \le S \le 0.3, \qquad \frac{S}{T_3^2} \le 0.405, \qquad T_3^2 \ge 0.18.$$

From the contour plot of the average-energy-consumption function E in Fig. 4, we obtain the energy-optimized step size S=0.20 m and time interval T_3=0.8 seconds, where the average-energy-consumption is 42 Nt. Figure 5 shows a sequence of the resulting stick diagrams (simulation) in the sagittal plane. The same walking parameters are used to experiment with the walking motions of the biped BR-1 as described in Section V.

IV. Motion Control

The servo control of the biped BR-1 consists of the computed gravity plus the PD compensator in the following form:

$$\boldsymbol{\tau} = \boldsymbol{g}(\boldsymbol{q}) + \boldsymbol{K}_p \boldsymbol{e} - \boldsymbol{K}_d \dot{\boldsymbol{q}}, \tag{26}$$

where $\boldsymbol{e} = \boldsymbol{q}_d - \boldsymbol{q}$, and $\boldsymbol{q}_d$ is the desired joint command. The asymptotic stability of dynamic equation Eq. (1) with control law Eq. (26) is based on fact that the matrix $(\dot{\boldsymbol{H}} - 2\boldsymbol{C})$ is skew-symmetric. The theorem (Lewis *et al.*, 1993) states the following:

> Suppose that the PD-gravity control law Eq. (26) is used in dynamic equation Eq. (1) and $\dot{\boldsymbol{q}}_d = 0$. The steady-state error $\boldsymbol{e} = \boldsymbol{q}_d - \boldsymbol{q}$ is, then, zero.

In particular, the proof is based on the positive-definite Lyapunov function

$$v(t) = \frac{1}{2}\dot{\boldsymbol{q}}^T \boldsymbol{H}(\boldsymbol{q})\dot{\boldsymbol{q}} + \frac{1}{2}\boldsymbol{e}^T \boldsymbol{K}_p \boldsymbol{e} \tag{27}$$

and its differentiation (Lewis *et al.*, 1993: 142)

$$\dot{v}(t) = -\frac{1}{2}\dot{\boldsymbol{q}}^T \boldsymbol{K}_d \dot{\boldsymbol{q}}. \tag{28}$$

In the following, we shall show that diagonal gain matrices $\boldsymbol{K}_p$ and $\boldsymbol{K}_d$ provide satisfactory performance. For a symmetric positive-definite matrix $\boldsymbol{A}$, the Rayleigh-Ritz Theorem states that

$$\lambda_{\min}(\boldsymbol{A})\boldsymbol{x}^T\boldsymbol{x} \le \boldsymbol{x}^T\boldsymbol{A}\boldsymbol{x} \le \lambda_{\max}(\boldsymbol{A})\boldsymbol{x}^T\boldsymbol{x},$$

where $\lambda_{\min}(\boldsymbol{A})$ and $\lambda_{\max}(\boldsymbol{A})$ denote the minimum and maximum eigenvalues of matrix $\boldsymbol{A}$, respectively. By the Rayleigh-Ritz Theorem, we have

$$\dot{v}(t) \le -\frac{1}{2}\lambda_{\min}(\boldsymbol{K}_d)\dot{\boldsymbol{q}}^T\dot{\boldsymbol{q}} \tag{29}$$

$$v(t) \le \frac{1}{2}h\dot{\boldsymbol{q}}^T\dot{\boldsymbol{q}} + \frac{1}{2}\lambda_{\max}(\boldsymbol{K}_p)b, \tag{30}$$

where h and b are constant bounds such that $h \ge \lambda_{\max}(\boldsymbol{H}(\boldsymbol{q}))$ and $b \ge \boldsymbol{e}^T\boldsymbol{e}$ in the region of interest. Rearranging (**30**), we obtain

$$-\dot{\boldsymbol{q}}^T\dot{\boldsymbol{q}} \le \frac{-2}{h}v(t) + \frac{\lambda_{\max}(\boldsymbol{K}_p)}{h}b. \tag{31}$$

Substituting the above inequality into Inequality (29), we obtain

$$\dot{v}(t) \le \frac{-2\lambda_{\min}(\boldsymbol{K}_d)}{h}v(t) + \frac{\lambda_{\min}(\boldsymbol{K}_d)\lambda_{\max}(\boldsymbol{K}_p)}{h}b. \tag{32}$$

Therefore, $v(t)$ is bounded by

$$v(t) \le c\exp\left(-\frac{2\lambda_{\min}(\boldsymbol{K}_d)}{h}t\right) + \frac{1}{2}\lambda_{\max}(\boldsymbol{K}_p)b \tag{33}$$

and

$$v(0) \le c + \frac{1}{2}\lambda_{\max}(\boldsymbol{K}_p)b, \tag{34}$$

where c is a constant to be determined later. From Inequality (30), we have

$$v(0) \le \frac{1}{2}h\dot{\boldsymbol{q}}(0)^T\dot{\boldsymbol{q}}(0) + \frac{1}{2}\lambda_{\max}(\boldsymbol{K}_p)b. \tag{35}$$

Comparing Inequalities (34) and (35), we can choose

$$c = \frac{1}{2}h\dot{\boldsymbol{q}}(0)^T\dot{\boldsymbol{q}}(0).$$

Therefore, $v(t)$ is bounded by

$$v(t) \le \frac{1}{2}h\dot{\boldsymbol{q}}(0)^T\dot{\boldsymbol{q}}(0)\exp\left(-\frac{2\lambda_{\min}(\boldsymbol{K}_d)}{h}t\right) + \frac{1}{2}\lambda_{\max}(\boldsymbol{K}_p)b. \tag{36}$$

Now, assume that $\boldsymbol{K}_p = \mathrm{diag}\{k_{p0}, \ldots, k_{p6}\}$ and $\boldsymbol{K}_d = \mathrm{diag}\{k_{d0}, \ldots, k_{d6}\}$, and that $\hat{\boldsymbol{K}}_p$ and $\hat{\boldsymbol{K}}_d$ are symmetric positive-definite matrices such that their diagonal elements are identical to $\boldsymbol{K}_p$ and $\boldsymbol{K}_d$ but contain non-zero off-diagonal elements. It is, then, not difficult to show that

$$\lambda_{\max}(\hat{\boldsymbol{K}}_p) \ge \lambda_{\max}(\boldsymbol{K}_p) > 0$$

and

$$0 < \lambda_{\min}(\hat{\boldsymbol{K}}_d) \le \lambda_{\min}(\boldsymbol{K}_d).$$

If one chooses PD gain matrices $\hat{\boldsymbol{K}}_p$ and $\hat{\boldsymbol{K}}_d$, the control law becomes

$$\boldsymbol{\tau} = \boldsymbol{g}(\boldsymbol{q}) + \hat{\boldsymbol{K}}_p\boldsymbol{e} - \hat{\boldsymbol{K}}_d\dot{\boldsymbol{q}},$$

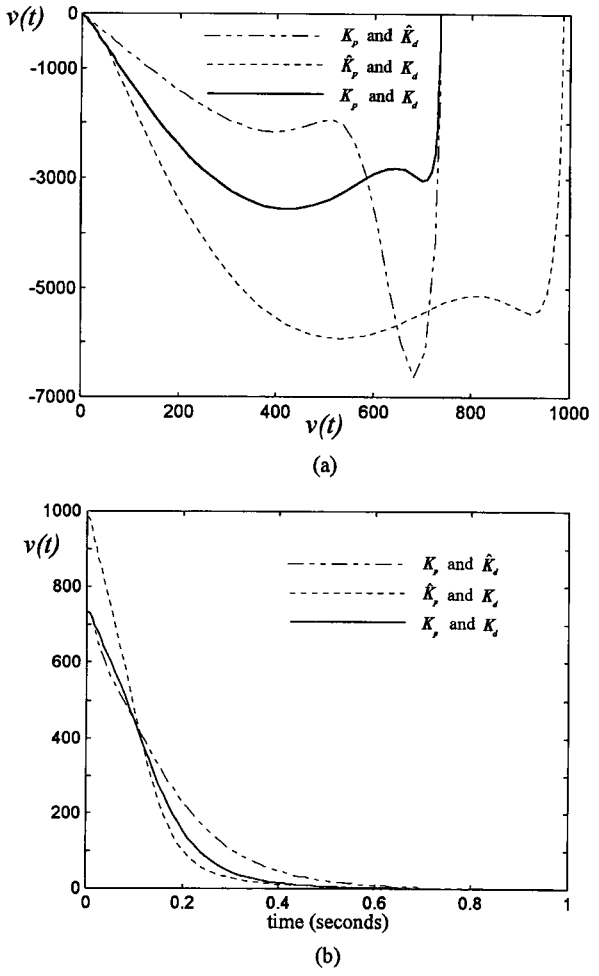

Fig. 6. Three Lyapunov functions with different gain matrices, in which K_p and K_d are diagonal matrices, $\hat{K}_p$ and $\hat{K}_d$ contain off-diagonal elements. (a) phase plane plots, (b) evolution of the Lyapunov functions.

and the corresponding Lyapunov function

$$\hat{v}(t)=\frac{1}{2}\dot{q}^T H(q)\dot{q}+\frac{1}{2}e^T\hat{K}_p e$$

is bounded by

$$\hat{v}(t)\le\frac{1}{2}h\dot{q}(0)^T\dot{q}(0)\exp(-\frac{2\lambda_{\min}(\hat{K}_d)}{h}t)+\frac{1}{2}\lambda_{\max}(\hat{K}_p)b\,. \quad (37)$$

Comparing Inequalities (36) and (37), we can conclude that the closed-loop system with diagonal PD gain matrices has a faster convergent rate and is less error bound. Therefore, to control a dynamic system in Eq. (1), local feedback at each joint may be used. Figure 6 displays simulation results of three evaluations of Lyapunov functions with different gain matrices. If the command is either a piecewise-constant trajectory or a continuous trajectory, the local PD-gravity feedback loop also can track well, provided that the velocity feedback gains are sufficiently large (Kawamura *et al.*, 1988).

Table 1. Biped BR-1's Physical Data

Joint	Initial Value	Joint Range	Actuator Gear Ratio	Maximum Torque/Force
d_0	0 cm	±13.5 cm	$1/14\pi$	291.6 Kgf
θ_1	0°	±28°	1/160	1.06×10^3 Kgf-cm
d_2	54.0 cm	±6.5 cm	$1/200\pi$	4166.0 Kgf
θ_3	0°	±36°	1/160	1.06×10^3 Kgf-cm
θ_4	0°	±28°	1/160	1.06×10^3 Kgf-cm
d_5	54.0 cm	±6.5 cm	$1/200\pi$	4166.0 Kgf
θ_6	0°	±36°	1/160	1.06×10^3 Kgf-cm

V. Experimental Walking

The prototype biped BR-1 has been designed and build at the National Taiwan Institute of Technology. The total height of the biped is 80 cm, and the total weight is about 42 kg. The foot size is 20 cm×15 cm. The two feet are separated by 5 cm. Each motor translates torque or force to the biped through a speed reducer. The physical data of the prototype biped are listed in Table 1. It is assumed that the frictional coefficient μ is large enough to prevent slippage between the supporting foot and the floor during walking.

The biped's motion control is designed to track a commanded path which is calculated in advance. The biped's motion control is realized by means of a hierarchical control structure, in which trajectory planning for the walking pattern is executed at the upper level, and the servo control for the planned trajectory is executed at the lower level. The servo control part is set up so as to follow the planned trajectory so that a stable walking motion is realized. The commanded joint trajectory for biped BR-1 is obtained by using a cubic B-spline data interpolation technique. First, each operation space command point is converted to a knot point in the joint space. Then, cubic B-spline trajectories which blend together the series of knots serve as the commanded joint position trajectories. The feedback gains are selected uniformly: k_{pi}=100 and k_{di}=9.23, for i=0, 1, ..., 6.

In dynamic walking experiments, the biped BR-1 moved forward and backward, including walk initiation, two continuous walking cycles, and walk termination, which were all recorded successfully on the video tape (Shih, 1996b). The limits on the travel distance were constrained by the length of the tether line connected to the off-board computer and drivers

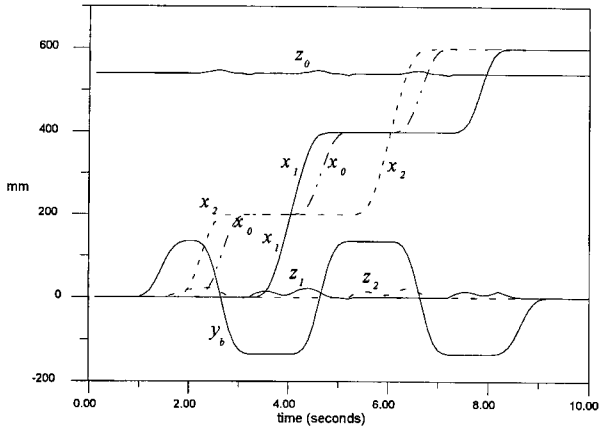

Fig. 7. The trajectory of the biped's body and two feet during experimental walking.

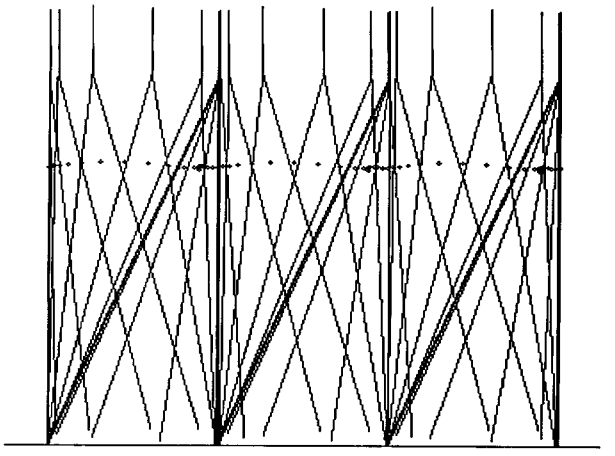

Fig. 8. Biped stick diagrams in the dynamic walking experiment. The small circles denote the center of gravity trajectory.

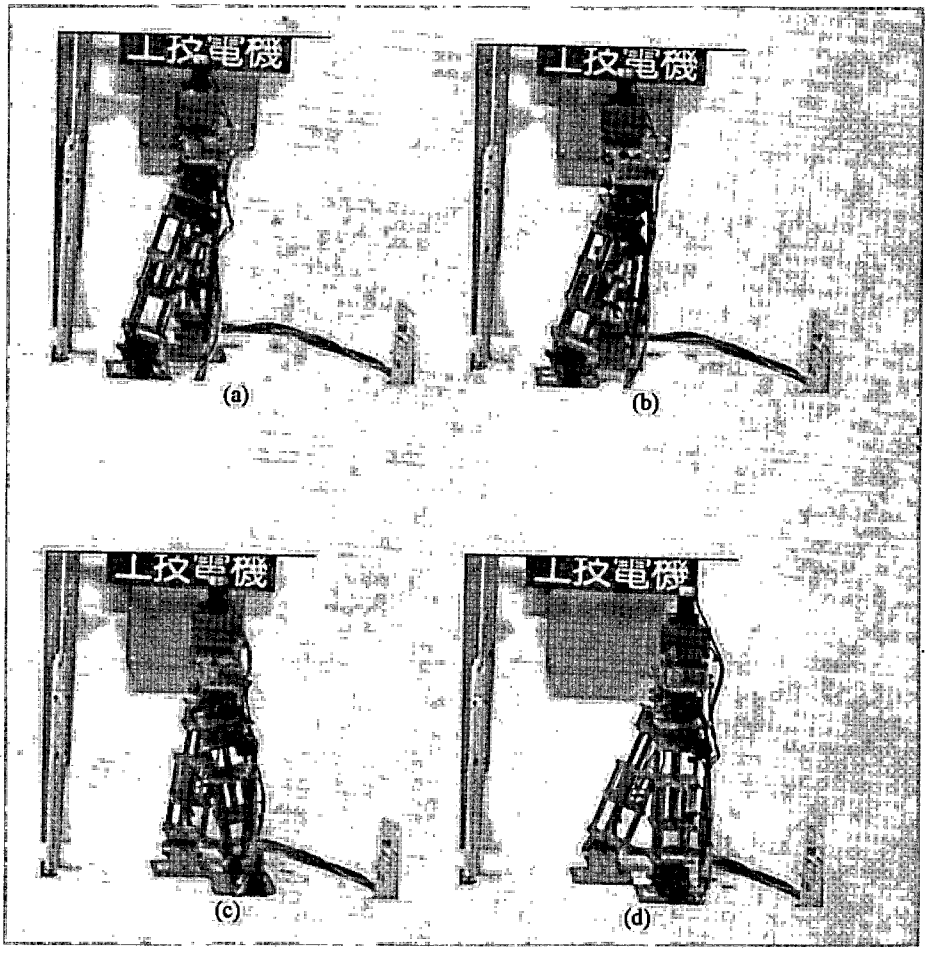

Fig. 9. Four pictures (a)-(d) taken during one walking cycle in the biped dynamic walking experiment.

rather than by the methodology itself. The main function of the balance weight was to lift up the swing foot at the beginning of the dynamic walking cycle. The walking pattern parameters were previously derived in Section III, where the step size S=0.20 m, h=0.03 m, W=0.15 m, T_1=0.4 seconds, δT=0.05 seconds and

T_2=T_3=0.8 seconds. Figure 7 shows the experimental operation trajectories during the dynamic walking experiment. Figure 8 shows a sequence of experimental stick diagrams in the sagittal plane. Except for the variations of the height of the swing feet, the experimental results are almost the same as the simulation result obtained previously. The downshift of the swing foot was mainly due to the gravity of the biped body, which contributed most of the weight of the biped. Figure 9 (a)-(d) shows a sequence of 4 pictures of the biped BR-1 during one complete walking cycle of the experiment.

During the dynamic walking experiment, the final speed and acceleration of the swing foot may not be zero; therefore, impact with the ground will occur. To overcome this problem, the speed of motion should not exceed a limit (e.g., 25 cm/s in our experiment), and it is required that the biped pause for a finite time interval before starting the next walking cycle. It has been shown that the main task of a biped is to slow down its motion at the end of a walking cycle and to finally reach a statically stable posture. To slow down the biped, a short pause between two continuous cycles is very effective, as occurred during the experiment. This short pause adds an additional impact phase to the walking cycle. Thus, as the biped walks, it still suffers from unsmooth motion (moving-and-resting motion) of the cg in the dynamic walking experiment. It is noted that zero velocity of the landing foot immediately after contact can be achieved by a shock-absorbing foot such as one with a rubber mat or an ankle that has flexibility for impact dumping with torque feedback sensors.

The proposed biped gait patterns are not optimal in the sense of speed and smoothness of trajectory; however, they are easy to implement. The proposed walking gaits can be transferred to the statically stable mode by placing the swing foot on the floor before the biped's body moves forward in Phase 3. Although the speed is slower when biped BR-1 walks in a statically stable manner, safer and less impact motion can be expected.

VI. Conclusions

In this study, we conducted a walking experiment on even floors with a biped robot BR-1 having seven degrees of freedom. The advantages of the biped BR-1 are: (1) it has simple kinematics and dynamics, and can be controlled by a local PD feedback loop; (2) its balance weight can effectively maintain balance of the center of gravity; and (3) a smooth and energy-optimized walking gait can be synthesized. The effectiveness of the proposed walking patterns for a biped walking on floors has been experimentally demonstrated. Future topics that need to be investigated include the dynamic walk of BR-1 on uneven terrain, such as stairs and sloping surfaces.

Acknowledgment

This work was supported by the National Science Council, R.O.C., under Grant NSC 85-2213-E-011-049.

References

Furusho, J. and M. Masubuchi (1986) Control of a dynamical biped locomotion system for steady walking. *ASME Journal of Dynamics, Systems, Measurement and Control*, **108**, 111-118.

Furusho, J. and A. Sano (1990) Sensor-based control of a nine-link biped. *International Journal of Robotics Research*, **9**, 83-98.

Grishin, A., A. Formal'sky, A. Lensky, and S. Zhitomirsky (1994) Dynamic walking of a vehicle with two telescopic legs controlled by two drivers. *International Journal of Robotics Research*, **13**, 137-147.

Kajita, S., T. Yamaura, and A. Kobayashi (1992) Dynamic walking control of a biped robot along a potential energy conserving orbit. *IEEE Trans. on Robotics and Automation*, **8**, 431-438.

Kawamura, S., F. Miyazaki, and S. Arimoto (1988) Is a local linear PD feedback control law effective for trajectory tracking of robot motion? *Proceeding 1988 IEEE International Conference on Robotics and Automation*, pp. 1335-1340. Philadelphia, PA, U.S.A.

Lewis, F., C. Abdallah, and D. Dawson (1993) *Control of Robot Manipulators*. Macmillan Publishing, New York, NY, U.S.A.

Li, Q., A. Takanishi, and I. Kato (1991) A biped walking robot having a ZMP measurement system using universal force-moment sensors. *IEEE/RSJ International Workshop on Intelligent Robots and Systems IROS '91*, pp. 1568-1573. Osaka, Japan.

Mita, T., T. Yamaguchi, T. Kashiwase, and T. Kawase (1984) Realization of a high speed biped using modern control theory. *International Journal of Control*, **40**, 107-119.

Miura, H. and I. Shimoyama (1984) Dynamic walk of biped locomotion. *International Journal of Robotics Research*, **3**, 60-74.

Miyazaki, F. and S. Arimoto (1980) A control theoretic study on dynamical biped locomotion. *ASME Journal of Dynamics, Systems, Measurement and Control*, **103**, 233-239.

Shih, C. L. (1996a) The dynamics and control of a biped walking robot with seven degrees of freedom. *ASME Journal of Dynamic Systems, Measurement, and Control*, **118**, 683-690.

Shih, C. L. (1996b) Experimental walking of a biped robot. *Video Proceeding 1996 IEEE International Conference on Industrial Electronics, Control, and Instrumentation, IECON'96*, p. 8. Taipei, Taiwan, R.O.C.

Vukobratovic, M.(1973) How to control artificial anthropomorphic systems. *IEEE Trans. on Systems, Man, and Cybernetics*, **3**, 497-507.

Zheng, Y. and F. Sias (1988) Design and motion control of practical biped robots. *International Journal of Robotics and Automation*, **3**, 70-77.

Dynamic Walking of a 7 DOF Biped Robot

二足步行機器人之動態步行實驗

施慶隆　薄占平

國立臺灣工業技術學院電機工程技術系

摘　要

本文實作一具能以動態平衡步行的二足步行機器人。此二足步行機器人有七個自由度，其機構主要包括兩個可伸縮的腳，及包含左右平移滑塊的身軀。其步行的方法是利用動力學，規劃並控制其身軀及雙腳之軌跡以保持平衡。本文主要的貢獻在於高效率、低能量之步行規劃，以及實驗的驗證。在平坦地面，此步行機能以每秒二十公分之速度運動。